

A mass-market Galileo receiver: Its algorithms and performance

*Original*

A mass-market Galileo receiver: Its algorithms and performance / Linty, NICOLA UMBERTO; Crosta, P.; Mattos, P.; Pisoni, F.. - In: GPS WORLD. - ISSN 1048-5104. - STAMPA. - 25:(2014), pp. 36-43.

*Availability:*

This version is available at: 11583/2556765 since:

*Publisher:*

Avanstar Communications

*Published*

DOI:

*Terms of use:*

This article is made available under terms and conditions as specified in the corresponding bibliographic description in the repository

*Publisher copyright*

(Article begins on next page)



# A Mass-Market Galileo Receiver

## Its Algorithms and Performance

The authors test three mass-market design drivers on a chip developed expressly for a new role as a combined GPS and Galileo consumer receiver: the time-to-first-fix for different C/N<sub>0</sub>, for hot, warm, and cold start, and for different constellation combinations; sensitivity in harsh environments, exploiting a simulated land mobile satellite multipath channel and different user dynamics; and power consumption strategies, particularly duty-cycle tracking.

Nicola Linty, Paolo Crosta, Philip G. Mattos, and Fabio Pisoni

**T**he two main GNSS receiver market segments, professional high-precision receivers and mass-market/consumer receivers, have very different structure, objectives, features, architecture, and cost. Mass-market receivers are produced in very high volume — hundreds of millions for smartphones and tablets — and sold at a limited price, and in-car GNSS systems represent a market of tens of millions of units per year. The reason for these exploding markets can be found not only in the improvements in electronics and integration, but also in the increasing availability of new GNSS signals. In coming years, with Galileo, QZSS, BeiDou, GPS-L1C, and GLONASS-CDMA all on the way, the silicon manufacturer must continue the path towards the fully flexible multi-constellation mass-market receiver.

Mass-market receivers feature particular signal processing techniques, different from the acquisition and

tracking techniques of standard GNSS receivers, in order to comply with mobile and consumer devices' resources and requirements. However, a limited documentation is present in the open literature concerning consumer devices' algorithms and techniques; besides a few papers, all the know-how is protected by patents, held by the main manufacturers, and mainly focused on the GPS L1 C/A signal. We investigate and prove the feasibility of such techniques by semi-analytical and Monte Carlo simulations, outlining the estimators sensitivity and accuracy, and by tests on real Galileo IOV signals.

To understand, analyze, and test this class of algorithms, we implemented a fully software GNSS receiver, running on a personal computer. It can process hardware- and software-simulated GPS L1 C/A and Galileo E1BC signals, as well as real signals, down-converted at intermediate frequency (IF), digitalized and

stored in memory by a front-end/bit grabber; it can also output standard receiver parameters: code delay, Doppler frequency, carrier-to-noise power density ratio ( $C/N_0$ ), phase, and navigation message. The software receiver is fully configurable, extremely flexible, and represents an important tool to assess performance and accuracy of selected techniques in different circumstances.

### Code-Delay Estimation

The code-delay estimation is performed in the software receiver by a parallel correlation unit, giving as output a multi-correlation with a certain chip spacing. This approach presents some advantages, mostly the fact that the number of correlation values that can be provided is thousands of times greater, compared to a standard receiver channel. Use of multiple correlators increases multipath-rejection capabilities, essential features in mass-market receivers, especially for positioning in urban scenarios. The multi-correlation output is exploited to compute the received signal code delay with an open-loop strategy and then to compute the pseudorange.

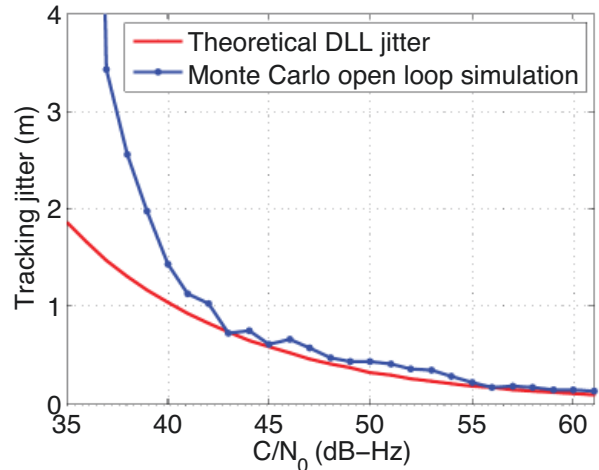
In the simulations performed, the multi-correlation has a resolution of 1/10 of a chip, which is equivalent to 30 meters for the signals in question; to increase the estimate accuracy, Whittaker-Shannon interpolation is performed on the equally spaced points of the correlation function belonging to the correlation peak.

The code-delay estimate accuracy is reported in FIGURES 1 and 2. The results are obtained with Monte Carlo simulations on simulated GNSS signals, with sampling frequency equal to 16.3676 MHz. In particular, a GPS L1 C/A signal is considered, affected by constant Doppler frequency equal to zero for the observation period, to avoid the effect of dynamics. The figures show the standard deviation of the code estimation error, that is, the difference between the estimated code delay and the true one, expressed in meters (pseudorange error standard deviation) for different values of  $C/N_0$ . To evaluate the quality of the results, the theoretical delay locked loop (DLL) tracking jitter is plotted for comparison, as

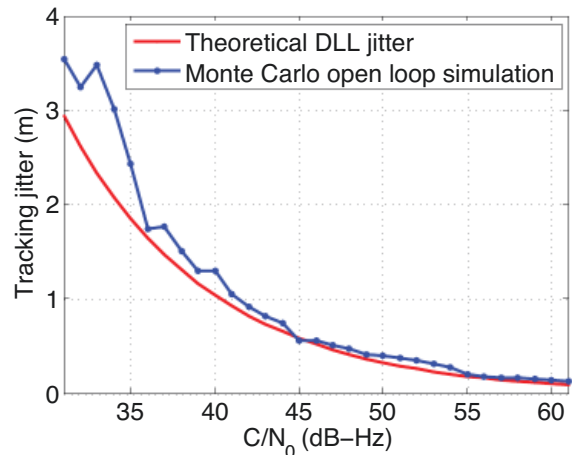
$$\sigma_{DLL} (m) = \sqrt{\frac{B_n}{2C/N_0} \left( \frac{R_c}{2B_{fe}} \right) \left( 1 + \frac{1}{T_c C/N_0} \right) \cdot \frac{c}{R_c}}$$

where  $B_n$  is the code loop noise bandwidth,  $R_c$  is the chipping rate,  $B_{fe}$  is the single sided front-end bandwidth,  $T_c$  is the coherent integration time, and  $c$  is the speed of light.

In the two figures, the red curve shows the theoretical tracking jitter for a DLL, which can be considered as term of comparison for code-delay estimation. To correlate the results, a E-L spacing equal to  $D = 0.2$  chip is chosen, and the code-delay error values of the software receiver simulation are filtered with a moving average filter. By averaging 0.5 seconds of data (for example,  $L = 31$  values spaced 16 milliseconds), an equivalent closed-loop



▲ FIGURE 1 Comparison between code delays estimation accuracy,  $T_c = 1$  ms,  $T = 16$  ms,  $B = 1$  Hz,  $D = 0.2$  chip.



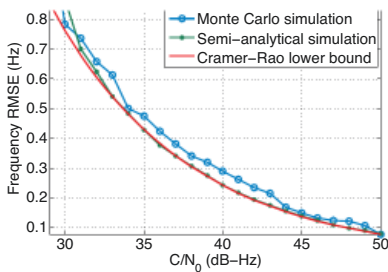
▲ FIGURE 2 Comparison between code delays estimation accuracy,  $T_c = 4$  ms,  $T = 64$  ms,  $B = 1$  Hz,  $D = 0.2$  chip.

bandwidth of about 1 Hz can be obtained:

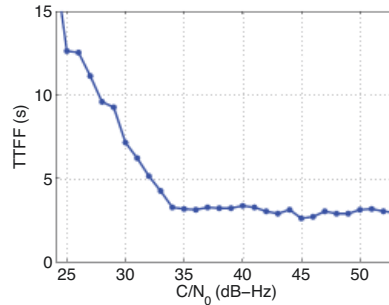
$$B = \frac{1}{2LT_c} = \frac{1}{2 \cdot 31 \cdot 0.016} \approx 1\text{ Hz}$$

In particular, in Figure 1, a coherent integration time equal to 1 millisecond (ms) and 16 non-coherent sums are considered, while in Figure 2 a coherent integration time equal to 4 ms and 16 non-coherent sums, spanning a total time  $T = 64$  ms, are considered. In both cases, the software receiver results are extremely good for high  $C/N_0$ . The code-delay error estimate is slightly higher than its equivalent in the DLL formulation. The open-loop estimation error notably increases in the first case below 40 dB-Hz due to strong outliers, whose probability of occurrence depends on the  $C/N_0$ . In fact, this effect is smoothed in the second case, where the coherent integration time is four times larger, thus improving the signal-to-noise ratio.

Nevertheless, the comparison between open loop multi-



▲ **FIGURE 3** Doppler frequency estimate RMSE versus  $C/N_0$  in super-high resolution with  $T=64$  ms, comparison between theoretical and simulated results.



▲ **FIGURE 4** Hot start TTFF for Galileo+GPS configuration versus  $C/N_0$  using the test receiver.

correlation approach and closed loop DLL is difficult and approximate, because the parameters involved are different and the results are only qualitative.

### Doppler Frequency Estimation

In the particular case of the software receiver developed here, the residual Doppler frequency affecting the GNSS signal is estimated by means of a maximum likelihood estimator (MLE) on a snapshot of samples, exploiting open-loop strategy. In fact, despite the higher standard deviation of the frequency error (jitter), open-loop processing offers improved tracking sensitivity, higher tracking robustness against fading and interference, and better stability when increasing the coherent integration time. In addition, the open-loop approach does not require the design of loop filters, avoiding problems with loop stability. A certain number of successive correlator values, computed in the multiple correlations block, are combined in a fast Fourier transform (FFT) and interpolated.

**FIGURE 3** shows the root mean square error (RMSE) of the frequency estimate versus signal  $C/N_0$ , obtained collecting 16 coherent accumulations of 4 ms of a Galileo E1B signal, then computing a 16 points FFT spanning a time interval of 64 ms, and finally refining the result with an interpolation technique. Three different curves are shown, corresponding respectively

to:

- the RMSE derived from simulations, carried out with GNSS data simulated with the N-FUELS signal generator;
- a semi-analytical estimation, exploiting the same algorithm;
- the Cramer-Rao lower bound (CRLB) for frequency estimation, shown as

$$CRLB = \frac{12}{(2\pi)^2 \cdot C/N_0/B_{fe} \cdot f_s \cdot T^3}$$

where  $f_s$  is the sampling frequency.

A well-known drawback is the so-called threshold effect. Below a certain  $C/N_0$ , the frequency estimate computed with MLE suffers from an error, and the RMSE increases with respect to the CRLB.

### Mass-Market Design Drivers

Once we have analyzed the features of some mass-market algorithms with a software receiver, we can move toward the performance of a real mass-market device, to compare results and confirm improvements brought by the new Galileo signals, so far mainly known from a theoretical point of view.

A recent survey identified three main drivers in the design of a mass-market receiver, coming directly from user needs, and solvable in different ways.

**Time-to-first-fix (TTFF)** corresponds to how fast a position, velocity, and time (PVT) solution is available

after the receiver is powered on, that is, the time that a receiver takes to acquire and track a minimum of four satellites, and to obtain the necessary information from the demodulated navigation data bits or from other sources.

**Capability in hostile environments**, for example while crossing an urban canyon or when hiking in a forest, is measured in terms of sensitivity. It can be verified by decreasing the received signal strength and/or adding multipath models.

**Power consumption** of the device. GNSS chipset is in general very demanding and can produce a not-negligible battery drain.

We analyzed these three drivers with a commercial mass-market receiver and with the software receiver.

### Open-Sky TTFF Analysis

TTFF depends on the architecture of the receiver, for example the number of correlators or the acquisition strategy, on the availability of assistance data, such as rough receiver position and time or space vehicles' (SV) ephemeris data, and on the broadcast navigation message structure. Some receivers, like the one used here for testing, embed an acquisition engine that can be activated on request and assures a low acquisition time; moreover, they implement ephemeris extension. In contrast, other consumer receiver manufacturers exploit a baseband-configurable processing unit, similar to the one implemented in the software receiver, with thousands of parallel correlators generating a multi-correlator output with configurable spacing, depending on the accuracy required. By selecting an appropriate number of correlators, depending on the available assistance data and on the accuracy required, the TTFF consequently varies.

We assessed the performance of the receiver under test for different

$C/N_0$ , for hot, warm, and cold start, and for different constellation combinations, exploiting hardware-simulated GNSS data. Good results are achieved, especially when introducing Galileo signals.

FIGURE 4 reports the hot-start TTFF for different  $C/N_0$  values in the range 25–53 dB-Hz, computed using the receiver. The receiver, connected to a signal generator, is configured in dual-constellation mode (GPS and Galileo) and carries out 40 TTFF trials, with a random delay between 15 and 45 seconds. In a standard additive white Gaussian noise (AWGN) channel and in hot-start conditions, the results mainly depend on the acquisition strategy and on the receiver availability of correlators and acquisition engines. In an ideal case with open-sky conditions and variable  $C/N_0$ , the introduction of a second constellation only slightly improves the TTFF performance; this result cannot be generalized since it mainly depends on the acquisition threshold of the receiver, which can change using signals of different constellations. In real-world conditions, the situation can vary.

**Cold Start.** Secondly, we analyze TTFF differences due to the different structure of GPS and Galileo navigation messages. The I/NAV message of the Galileo E1 signal and the data broadcast by GPS L1 C/A signals contain data related to satellite clock, ephemeris, and GNSS time: parameters relevant to the position fix since they describe the position of the satellite in its orbit, its clock error, and the transmission time of the received message.

TABLE 1 shows some results in the particular case of cold start, with an ideal open-sky AWGN scenario. The TTFF is significantly lower when using Galileo satellites: while the mean TTFF when tracking only GPS satellites is equal to about 31.9 seconds (s), it decreases to 24.7 s when considering only Galileo satellites, and to 22.5 s in the case of dual constellation. Similarly, the minimum and maximum TTFF values are lower when tracking Galileo satellites. The 95 percent probability values confirm the theoretical expectations. Again, in the ideal case with open-sky conditions, the results with two constellations are quite similar to the performance of the signal with faster TTFF. However, in non-ideal conditions, use of multiple constellations represents a big advantage and underlines the importance of developing at least dual-constellation mass-market receivers.

Furthermore, it is interesting to analyze in more detail the case of a GPS and Galileo joint solution. GPS and Galileo system times are not synchronized, but differ by a small quantity, denoted as the GPS-Galileo Time Offset (GGTO). When computing a PVT solution with mixed signals, three solutions are possible: to estimate it as a fifth unknown, to read it from the navigation message, or to use pre-computed value. In the first case it is not necessary to rely on the information contained

	<i>min</i>	<i>Max</i>	<i>Mean</i>	<i>95%</i>
GPS	22.2	40.1	31.9	36.2
Galileo	18.6	36.6	24.7	32.3
GPS+Galileo	19.6	35.4	22.5	31.9

▲ **TABLE 1** Comparison between TTFF (in seconds) in cold start for different constellation combinations.

in the navigation message, eventually reducing the TTFF. However, five satellites are required to solve the five unknowns, and this is not always the case in urban scenarios or harsh environments, as will be proved below. On the contrary, in the second case, it is necessary to obtain the GGTO information from the navigation message, and since it appears only once every 30 seconds, in the worst case it is necessary to correctly demodulate 30 seconds of data. Both approaches show benefits and disadvantages, depending on the environment. The receiver under test exploits the second solution: in this case, it is possible to see an increase in the average TTFF when using a combination of GPS and Galileo, due to the demodulation of more sub-frames of the broadcast message.

**MAXTENA**  
WIRELESS INNOVATIONS COMPANY

**GPS HELIX ANTENNAS**  
BUILT ON ADVANCED HELICORE® TECHNOLOGY

Maxtena designs and builds high performance multiband antennas for GNSS, M2M, MSS, & LTE applications.

Tel: 1-844-505-7053 - Email: [contact@maxtena.com](mailto:contact@maxtena.com) - [www.maxtena.com](http://www.maxtena.com)

	<i>min</i>	<i>Max</i>	<i>Mean</i>
<b>HOT start</b>	4.5	12.4	7.9
<b>WARM start</b>	31.5	67.2	36.3
<b>COLD start</b>	40.5	265.7	105.0

▲ **TABLE 2** TTFF (in seconds) exploiting GPS and Galileo constellations in harsh environments.

**Sensitivity: Performance in Harsh Environments**

Harsh environment is the general term used to describe those scenarios in which open sky and ideal propagation conditions are not fulfilled. It can include urban canyons, where the presence of high buildings limits the SV visibility and introduces multipath; denied environments, where unintentional interference may create errors in the processing; or sites where shadowing of line-of-sight (LoS) path is present, for example due to trees, buildings, and tunnels. In these situations it is necessary to pay particular attention to the signal-processing stage; performance is in general reduced up to the case in which the receiver is not able to compute a fix.

A first attempt to model such an environment has been introduced in the 3GPP standard together with the definition of A-GNSS minimum performance requirements for user equipment supporting other A-GNSSs than GPS L1 C/A, or multiple A-GNSSs which may or may not include GPS L1 C/A. The standard test cases support up to three different constellations; in dual-constellation case it foresees three satellites in view for each constellation with a horizontal dilution of precision (HDOP) ranging from 1.4 to 2.1.

To perform TTFF and sensitivity tests applying the 3GPP standard test case, we configured a GNSS simulator scenario with the following characteristics, starting from the nominal constellation:

- Six SVs: three GPS (with PRN 6,7, 21) and three Galileo (with code number 4, 11, 23);
- HDOP in the range 1.4 – 2.1;
- nominal power as per corresponding SIS-ICD;
- user motion, with a heading direction towards 90° azimuth, at a constant speed of 5 kilometers/hour (km/h).

In addition to limiting the number of satellites, we introduced a narrowband multipath model. The multi-SV two-states land mobile satellite (LMS) model simulator generated fading time series representative of an urban environment. The model includes two states:

- a good state, corresponding to LOS condition or light shadowing;
- a bad state, corresponding to heavy shadowing/blockage.

Within each state, a Loo-distributed fading signal is assumed. It includes a slow fading component (lognormal fading) corresponding to varying shadowing conditions

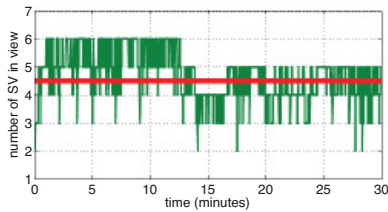
of the direct signal, and a fast fading component due to multipath effects. In particular, the last version of the two-state LMS simulator is able to generate different but correlated fading for each single SV, according to its elevation and azimuth angle with respect to the user position: the angular separation within satellites is crucial, since it affects the correlation of the received signals. This approach is based on a master–slave concept, where the state transitions of several slave satellites are modeled according to their correlation with one master satellite, while neglecting the correlation between the slave satellites. The nuisances generated are then imported in the simulator scenario, to timely control phase and amplitude of each simulator channel. Using this LMS scenario, the receiver’s performance in harsh environments has been then verified with acquisition (TTFF) and tracking tests.

The TTFF was estimated with about 50 tests, in hot, warm, and cold start, first using both GPS and Galileo satellites, and then using only one constellation. In the second case only the 2D fix is considered, since, according to the scenario described, at maximum three satellites are in view. **TABLE 2** reports the results for the dual-constellation case: in hot start the average TTFF is about 8 s, and it increases to 36 s and 105 s respectively for the warm and cold cases. Clearly the results are much worse than in the case reported earlier of full open-sky AWGN conditions. In this scenario only six satellites are available at maximum; moreover, the presence of multipath and fading affects the results, and they exhibit a larger variance, because of the varying conditions of the scenario.

**TABLE 3** shows similar results, but for the GPS-only case. In this case the receiver was configured to track only GPS satellites. The mean TTFF increases both in the hot and in the warm case, whereas in cold start it is not possible compute a 2D fix with only three satellites; the ambiguity of the solution cannot be solved if an approximate position solution is not available. It may seem unfair to compare a scenario with three satellites and one with six satellites. However, it can be assumed that this is representative of what happens in limited-visibility conditions, where a second constellation theoretically

	<i>min</i>	<i>Max</i>	<i>Mean</i>
<b>HOT start</b>	4.7	38.0	11.8
<b>WARM start</b>	31.6	109.7	51.9
<b>COLD start</b>	N.A. (*)	N.A. (*)	N.A. (*)
* 4 SVs required for cold start			

▲ **TABLE 3** TTFF (in seconds) exploiting only GPS constellations in harsh environments.

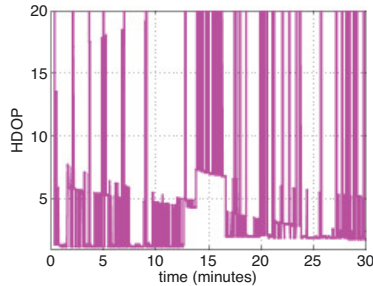


▲ **FIGURE 5** Number of satellites tracked by the test receiver in the Multi-SV LMS simulation.

doubles the number of satellites in view.

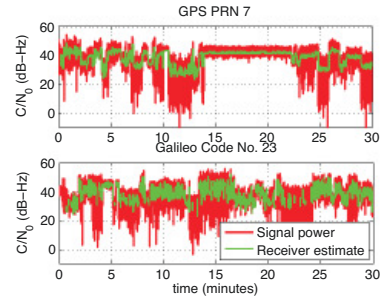
The results confirm the benefits of dual-constellation mass-market receivers in harsh environments where the number of satellites in view can be very low. Making use of the full constellation of Galileo satellites will allow mass-market receivers to substantially increase performances in these scenarios.

**Tracking.** We carried out a 30-minute tracking test with both the receiver



▲ **FIGURE 6** HDOP computed by the test receiver in the Multi-SV LMS simulation.

and the software receiver model. Both were able to acquire the six satellites and to track them, even with some losses of lock (LoLs) due to fading and multipath reflections. **FIGURE 5** shows the number of satellites in tracking state in the receiver at every second, while **FIGURE 6** shows the HDOP as computed by the receiver. When all six satellites are in tracking state, the HDOP lies in the range 1.4 – 2.1, as



▲ **FIGURE 7**  $C/N_0$  estimate computed by the receiver in harsh environments and compared with the signal power.

defined in the simulation scenario; on the contrary, as expected, in correspondence with a LoL it increases.

**FIGURE 7** compares the signal power generated by the simulator and the power estimated by the receiver, in the case of GPS PRN 7 and Galileo code number 23. This proves the tracking capability of the receiver also for high sensitivity. To deal with



**AUVSI's**  
Unmanned Systems  
**2014**

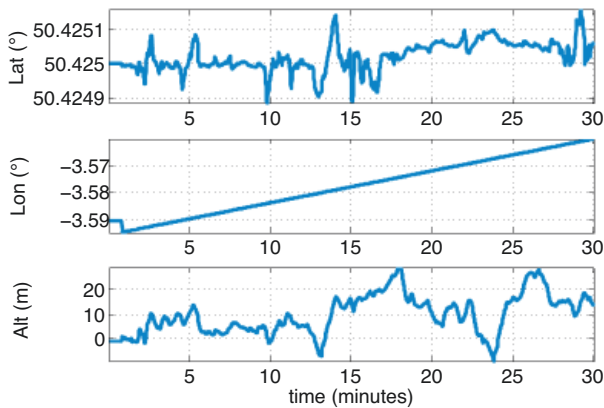
**CONFERENCE 12-15 MAY**  
**TRADE SHOW 13-15 MAY**

**ORANGE COUNTY CONVENTION CENTER**  
**ORLANDO, FLA. | USA**

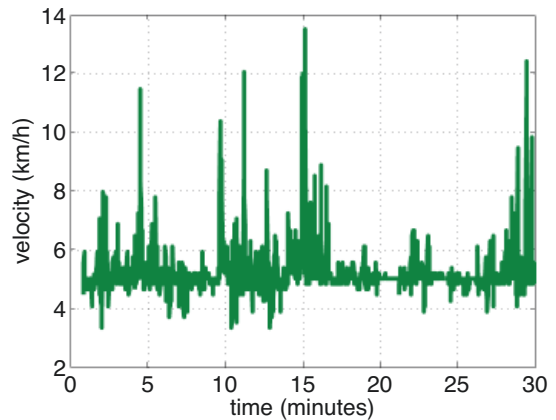
# REGISTER TODAY



**AUVSISHOW.ORG**



▲ **FIGURE 8** Test receiver position solution in LMS scenario.



▲ **FIGURE 9** Test receiver velocity solution in LMS scenario.

low-power signals, the integration time is extended both for GPS and for Galileo, using the pilot tracking mode in the latter case.

FIGURES 8 and 9 show respectively the position and the velocity solution. In the first case latitude, longitude, and altitude are plotted, while in the second case the receiver speed estimate in km/h is reported.

In this framework it is possible to evaluate the advantages and disadvantages of using the broadcast GGTO when computing a mixed GPS and Galileo position. When the LMS channel conditions are good, all six SVs in view are in tracking state, as shown in Figure 5. However, when the fading becomes important, the number is reduced to only two satellites. If the receiver is designed to extract the GGTO from the navigation message, then a PVT solution is possible also when only four satellites are in tracking state, that is for 90 percent of the time in this specific case. On the contrary, if the GGTO has to be estimated, one more satellite is required, and this condition is satisfied only 57 percent of the time, strongly reducing the probability of having a fix. Nevertheless, estimating the GGTO requires the correct demodulation of the navigation message, and this is possible only if the signal is good enough for a sufficient time.

### Power-Saving Architectures

The final driver for mass-market receivers design is represented by power consumption. Particularly for chips suited for portable devices running on batteries, power drain represents one of the most important design criteria. To reduce at maximum the power consumption, chip manufacturers have adopted various solutions. Most are based on the concept that, contrarily to a classic GNSS receiver, a mass-market receiver is not required to constantly compute a PVT solution. In fact, most of the time, GNSS chipsets for consumer devices are only required to keep updated information on approximate time and position and to download clock corrections and ephemeris data with a proper time rate, depending on the navigation message type and the adopted extended ephemeris algorithm. Then, when asked, the receiver can quickly provide a position fix. By reducing the computational load of the device during waiting mode, power consumption is reduced proportionally.

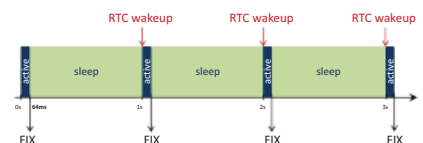
To better understand advantages and disadvantages of power saving techniques, some of them have been studied and analyzed in detail. In particular, the algorithm implemented in the software receiver model is based on two different receiver states: an active state, in which all receiver parts are activated, as in a standard

receiver, and a sleep state, where the receiver is not operating at all. In the sleep state, the GNSS RF module, GNSS baseband, and digital signal processor core are all switched off. By similarity to a square wave, these types of tracking algorithms are also called duty-cycle (DC) algorithms. Exploiting the software approach's flexibility, we can test the effect of two important design parameters:

- sleep period length;
- minimum active period length.

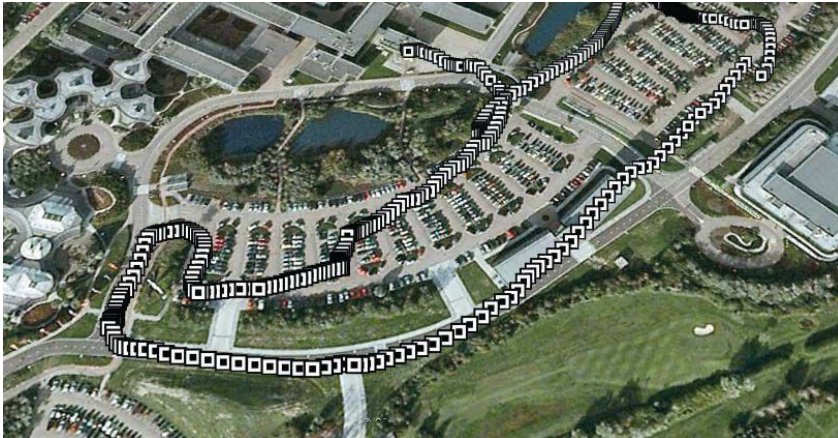
Their setting is not trivial and depends on the channel conditions, on the signal strength, on the number of satellites in view, on the user dynamics, and finally on the required accuracy.

In the software receiver simulations performed, the active mode length is fixed to 64 ms: the receiver collects 16 correlation values with coherent integration time equal to 4 ms, to perform frequency estimation as described above. Then it switches to sleep state for 936 ms, until a real-time clock (RTC) wake-up initiates the next full-power state. In this way a fix is available at the rate



▲ **FIGURE 10** Duty cycle tracking pattern in the software receiver simulations.





▲ **FIGURE 11** Galileo-only mobile fix, computed on March 12, 2013.

of 1 s, as summarized in **FIGURE 10**. However, there are some situations where the receiver may stay in full-power mode, for example during the initialization phase, to collect important data from the navigation message, such as the ephemeris, and to perform RTC calibration.

There are benefits of using this approach coupled to Galileo signals: the main impact is the usage of the pilot codes. Indeed, a longer integration time allows reducing the active period length, which most impacts the total power consumption, being usually performed at higher repetition rate.

Some simulations were carried out to assess the performance of DC algorithms in the software receiver. While in hardware implementations the direct benefit is the power computation, in a software implementation it is not possible to see such an improvement. The reduced power demand is translated into a shorter processing time for each single-processing channel. The DC approach can facilitate the implementation of a real-time or quasi-real-time software receiver.

The main drawback of using techniques based on DC tracking is the decrease of the rate of observables and PVT solution. However, this depends on the application; for some, a solution every second is more than enough.

### Real-Signal Results

On March 12, 2013, for the first time the four Galileo IOV satellites were broadcasting a valid navigation message at the same time. From 9:02 CET, all the satellites were visible at ESTEC premises, and the first position fix of latitude, longitude, and altitude took place at the TEC Navigation Laboratory at ESTEC (ESA) in Noordwijk, the Netherlands. At the same time, we were able to acquire, track, and compute one of the first Galileo-only mobile navigation solutions, using the receiver under test. Thanks to its small size and portability, it was installed on a mobile test platform, embedded in ESA's Telecommunications and Navigation Testbed vehicle. Using a network connection, we could follow, from the Navigation Lab, the real-time position of the van moving around ESTEC.

**FIGURE 11** shows the van's track, obtained by post processing NMEA data stored by the receiver evaluation board. The accuracy achieved in these tests met all the theoretical expectations, taking into account the limited infrastructure deployed so far. In addition, the results obtained with the receiver have to be considered preliminary, since its firmware supporting Galileo was in an initial test phase (for example, absence of a proper ionospheric model, E1B-only tracking).

### Conclusions

Analysis of a receiver's test results confirms the theoretical benefits of Galileo OS signals concerning TTFF and sensitivity. Future work will include the evolution of the software receiver model and a detailed analysis of power-saving tracking capabilities, with a comparison of duty-cycle tracking techniques in open loop and in closed loop.

### Acknowledgments

This article reflects solely the authors' views and by no means represents official European Space Agency or Galileo views. The article is based on a paper first presented at ION GNSS+ 2013. Research and test campaigns related to this work took place in the framework of the ESA Education PRESTIGE programme, thanks to the facilities provided by the ESA TEC-ETN section. The LMS multipath channel model was developed in the frame of the MiLADY project, funded by the ARTES5.1 Programme of the ESA Telecommunications and Integrated Applications Directorate.

### Manufacturers

The tests described here used the **STMicroelectronics** ([www.st.com/gps](http://www.st.com/gps)) Teseo II receiver chipset and a **Spirit** ([www.spirent.com](http://www.spirent.com)) signal simulator.

**NICOLA LINTY** is a Ph.D. student in electronics and telecommunications at Politecnico di Torino. In 2013 he held an internship at the European Space Research and Technology Centre of ESA.

**PAOLO CROSTA** is a radio navigation system engineer at the ESA TEC Directorate where he provides support to the EGNOS and Galileo programs. He received a MSc degree in telecommunications engineering from the University of Pisa.

**PHILIP G. MATTOS** received an external Ph.D. on his GPS work from Bristol University. He leads the STMicroelectronics team on L1C and BeiDou implementation, and the creation of totally generic hardware that can handle even future unknown systems.

**FABIO PISONI** has been with the GNSS System Team at STMicroelectronics since 2009. He received a master's degree in electronics from Politecnico di Milano, Italy.